Surface/Interfacial Changes During Polyurethane Crosslinking: A Spectroscopic Study. V*

QIWEN HAN, MAREK W. URBAN

The University of Southern Mississippi, School of Polymers and High Performance Materials, Shelby F. Thames Polymer Research Center, Hattiesburg, Mississippi 39406

Received 2 May 2000; accepted 30 May 2000

ABSTRACT: Crosslinking reactions and stratification processes in polyurethane films were investigated using attenuated total reflectance (ATR) FTIR spectroscopy. The HDI trimer levels near the film–substrate (F–S) interface appear to increase at the early stages of reactions, and after reaching a maximum, decrease. This is attributed to solvent depletion and subsequent film shrinkage, thus causing local NCO concentration changes. At the later stages of crosslinking reactions, stratification of the 1,6-hexamethylene diisocyanate (HDI) trimer occurs, with higher concentration levels at shallower penetration depths from the F–S interface. At the same time, NCO-containing groups assume preferentially parallel orientation to the F–S interface. On the other hand, H-bonded carbonyl groups tend to orient themselves in a perpendicular direction. Quantitative analysis indicates that at extended reaction times the amount of H-bonded C═O groups at shallower penetration depths increases and their orientation tends to be more random, which is correlated with migration toward the F–S interface.
 J Appl Polym Sci 81: 2045–2054, 2001

Key words: polyurethanes; crosslinking; surfaces/interfaces; spectroscopy

INTRODUCTION

Although there have been numerous studies conducted on polyurethanes (PURs),[1–6] the issue of surface/interfacial stratification is relatively new. As a matter of fact, it was not until 1996 that the first study concerned with NCO stratification was published and showed that humidity and crosslinking conditions significantly affect PUR film formation.[7] Other studies also recognized that kinetics[8] and surface morphology[9] are affected by environmental conditions, particularly, by the presence of water. Recent quantitative studies[10–12] also indicated that, in addition to the NCO sensitivity to water, there are other important surface/interfacial features. For example, one would anticipate that, due to the consumption of NCO functionalities during crosslinking reactions, NCO concentration levels would decrease as polyol–1,6-hexamethylene diisocyanate (HDI) reactions progress. However, experimental evidence showed that there are circumstances where the NCO concentration initially increases during crosslinking, followed by its decline.[10,11] To understand this phenomenon, we expanded the scope of the previous studies and examined factors that may influence this behavior. Previous studies[10,12] also showed that NCO groups orient randomly near the film–substrate (F–S) interface, no NCO stratification occurs at the early stages of reactions, and H-bonded C═O groups ex-

* Parts I–IV were published in the *Journal of Coating Technology*.

Correspondence to: M. W. Urban.

Contract grant sponsors: National Science Foundation Industry/University Cooperative Research Center in Coatings; Bayer Corp.

Journal of Applied Polymer Science, Vol. 81, 2045–2054 (2001)

hibit a preferentially perpendicular direction to the F–S interface. Since functional-group changes and H-bonding play an important role in PUR film formation at various depths from the surface, this study also addressed transient interfacial changes occurring during film formation.

EXPERIMENTAL

Hydroxy1-substituted polyacrylate Desmophen A-450A (50% (w/w) solids in a 50:50 (w/w) xylene and butyl acetate solvent mixture) and the HDI trimer (Desmodur N3300) were obtained from the Bayer Co. Anhydrous xylene (99+%) and anhydrous butyl acetate (99+%) were purchased from the Aldrich Chemical Co., Inc. Acrylic polyol and the isocyanurate crosslinker were mixed in a 1:1.1 [OH]/[NCO] ratio. The mixture was stirred for 2 min and drawn onto a substrate (typically Ge) to yield a wet film with thickness of 200 ± 10 μm. Such prepared films were allowed to crosslink at 25°C and 7% relative humidity (RH).

Transmission and attenuated total reflectance (ATR) FTIR spectra were collected on a Nicolet Magna-IR® 850 spectrometer. An ATR variable-angle multiple-reflection attachment (Spectra Tech, Inc.) with a 45° end parallelogram KRS-5 or Ge crystal was utilized. The spectrometer was continuously purged with dry air supplied from a Balston type 75–60 air-purification system. A Graseby Specac 12000 polarizer was used to determine the preferential orientation of the functional groups. Each spectrum was collected at a 4-cm^{-1} resolution and represented 200 co-added scans, collected and ratioed against a background of 200 co-added scans of an empty ATR cell equipped with KRS-5 or Ge crystals. In an effort to vary the depth of penetration into the films, the ATR attachment was aligned at various angles of incidence. Concentration levels of isocyanate were determined by constructing a calibration curve which allowed us to correlate the band intensity at 2273 cm^{-1} to the NCO concentration. In an effort to eliminate optical effects resulting from the dispersive nature of the ATR measurements, all spectra were corrected using Q-ATR software.[13] Spectral features of overlapping bands were deconvoluted using a maximum entropy approach.[14]

RESULTS AND DISCUSSION

As in the previous studies,[7–12] ATR FTIR spectroscopy was utilized to follow molecular level changes resulting from crosslinking reactions of the HDI trimer and acrylic polyol. Tentative band assignments for polyacrylate, isocyanate, and the resulting PUR are summarized in Table I.[10–15] Here, we just point out the bands that are responsible for crosslinking reactions and structural features occurring during PUR film formation near the film–air (F–A) and film–substrate (F–S) interfaces. Figure 1 shows ATR FTIR spectra of PUR collected from the F–S interface, and traces A, B, and C represent the spectra measured after 1, 8, and 38 h, respectively, of reactions conducted under 5–10% RH. Of particular interest is the band due to NCO functionality at 2273 cm^{-1} because its intensity is proportional to the concentration changes of the NCO groups. The band at 1730

Table I FTIR Band Assignments for PUR Components

Band	Wavenumber (cm^{-1}) Acrylic Polyol	HDI Trimer	PUR
C—OH str.	3532		3532
N—H str.			3395
Overtone C═O	3214		
ν_a CH_3	2961		
ν_a CH_2		2939	2936
ν_s CH_2	2890	2864	2863
NCO out of phase		2273	2273
Free C═O str.		1760	1780
Acrylic C═O str.	1730		1730
Urea C═O str.		1690	1690
δ N—H and ν_a C—N amide II (urea)			~ 1525
δ CH_2	1464	1465	1464
NCO in phase str.		1430	1427
δ —C(CH_3)	1386	1374	1374
NCO in-phase		1340	1335
CH_2 twist	1302	1304	1304
(O═)C—O—C str.	1150		1150
ν_a C—N—C	1146	1143	
ν_a C—O—C			1097
C—C skel vib.	1055	1048	1058
C—C—O out of phase	996		994
C—C skel. vib.		952	942
ν_s C—N—C		861	856
ν_s C—O—C	829		828
C—C—O in phase			766
CH_2 in-phase-rock	729	732	731
δ NCO		583	
δ C—O—C			428

ν_s, symmetric stretch; ν_a, asymmetric stretch; δ, deformation.

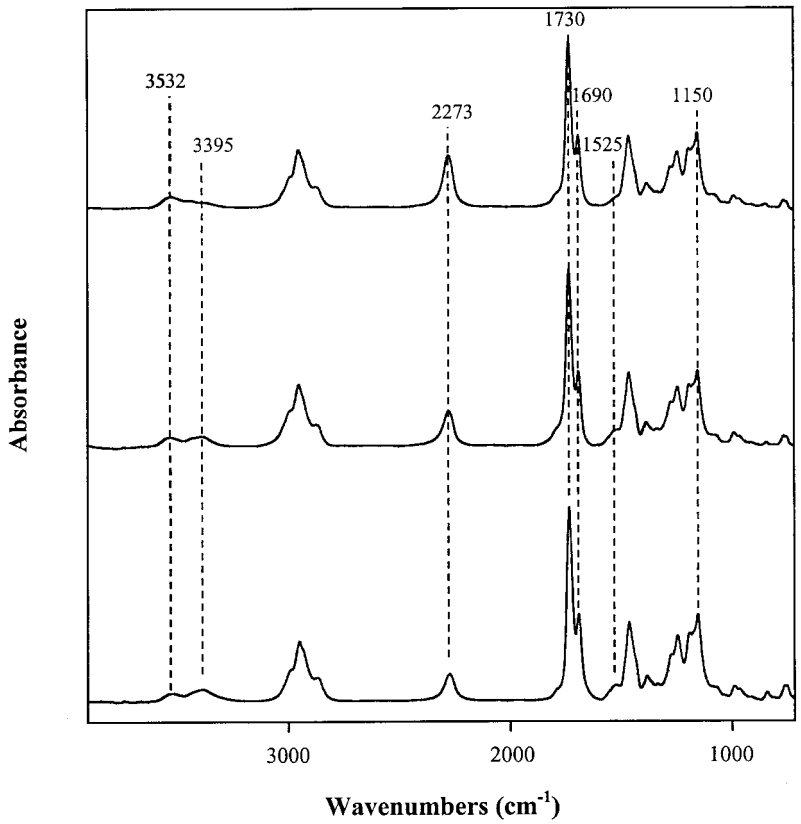

Figure 1 ATR FTIR spectra of solvent-borne PUR recorded at the F–S interface at 7% RH and 25°C for reaction times of (A) 1 h, (B) 8 h, and (C) 38 h.

cm^{-1} is due to acrylic carbonyl (C═O) groups, and the 1690-cm^{-1} band is due to C═O groups of urea of the HDI trimer.[10,11] Comparison of traces A, B, and C in Figure 1 indicates that, as the reactions proceed, the intensity of the 2273-cm^{-1} band decreases since NCO groups are consumed. At the same time, the band at 3532 cm^{-1}, corresponding to the O—H stretching modes in acrylic polyol, and the band at 1242 cm^{-1}, due to O═C—O—C stretching vibrations of the butyl acetate solvent, decrease. In contrast, the bands due to urethane linkages, including N—H stretching and deformation bands at 3395 and 1525 cm^{-1}, respectively, and the (O═)C—O—C stretching band at 1150 cm^{-1}, increase as crosslinking reactions progress.

Following the intensity changes of the 2273-cm^{-1} band, the NCO concentration changes near the F–A and F–S interfaces under different crosslinking conditions can be monitored by determination of the NCO extinction coefficient.[11] As shown in Figure 2, curve A, as the reaction progresses, NCO concentrations at the early stages of reactions reach a maximum; that is, during the first 1–2 h, the NCO concentration near the F–S interface increases, followed by its decrease. This behavior at the early stages of the reactions is somewhat surprising, as one would expect consumption of the NCO groups during the entire process. However, solvents may play an important role at the early stages of the reactions. Curve B of Figure 2 shows solvent depletion plotted as a function of time and it appears that, within the first 1–2 h of crosslinking, the solvent evaporates rapidly, which parallels the increase of the NCO concentration. These observations indicate that, at the early stages of the reactions, solvent evaporation, which leads to an increase of the NCO concentration, is the controlling factor for the NCO concentration changes. After 1–2 h of the reactions, solvent evaporation slows down and the consumption of NCO groups due to crosslinking reactions becomes the controlling factor. It should be also noted that Figure 2, curve B, represents the weight loss of two solvents: butyl acetate and xylene.

In an effort to determine contributions of each solvent to the mixture, concentration changes of

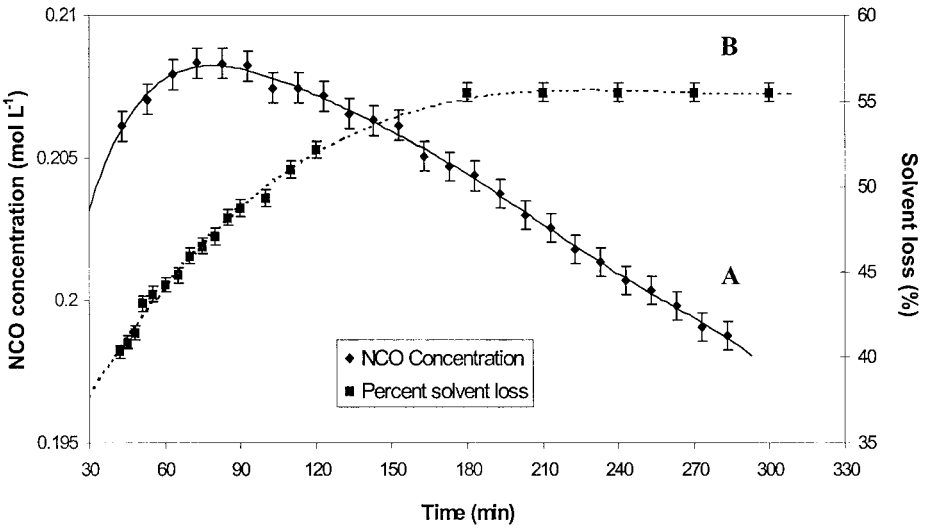

Figure 2 (A) NCO concentration of solvent-borne PUR at 0.29-μm depth from the F–S interface and (B) percent solvent loss as the functions of reaction time recorded under 7% RH.

both solvents as a function of time near the F–S interface using ATR FTIR spectroscopy was monitored. While Figure 3, curves A and B, compare individual butyl acetate and xylene concentration changes within the film, curve C shows the total solvent loss. As seen, both solvents exhibit the same desorption patterns, which parallel the solvent mixture evaporation curve, indicating that neither butyl acetate nor xylene partial vapor pressures dominate the evaporation process.

Previous studies indicated that the NCO concentration changes as a function of distance from the F–A and F–S interfaces.[11] In an effort to examine if NCO groups exhibit preferential orientation at various distances from the surface, ATR FTIR measurements were employed by varying the angle of incidence and using polarized light. The use of polarized light allows us to determine the orientation of functional groups.[16] Following the accepted convention, the transverse electric (TE) wave of infrared radiation is defined as having its electric vector parallel to the crystal plane (or perpendicular to the plane of incidence), whereas the transverse magnetic (TM)

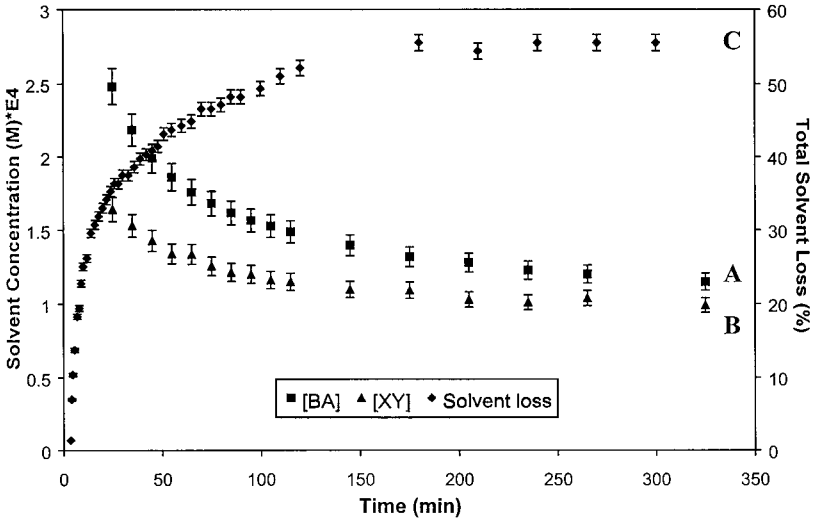

Figure 3 (A) Butyl acetate and (B) xylene concentration at 0.3 μm depth of penetration from the F–S interface and (C) total solvent loss of the PU film as a function of time.

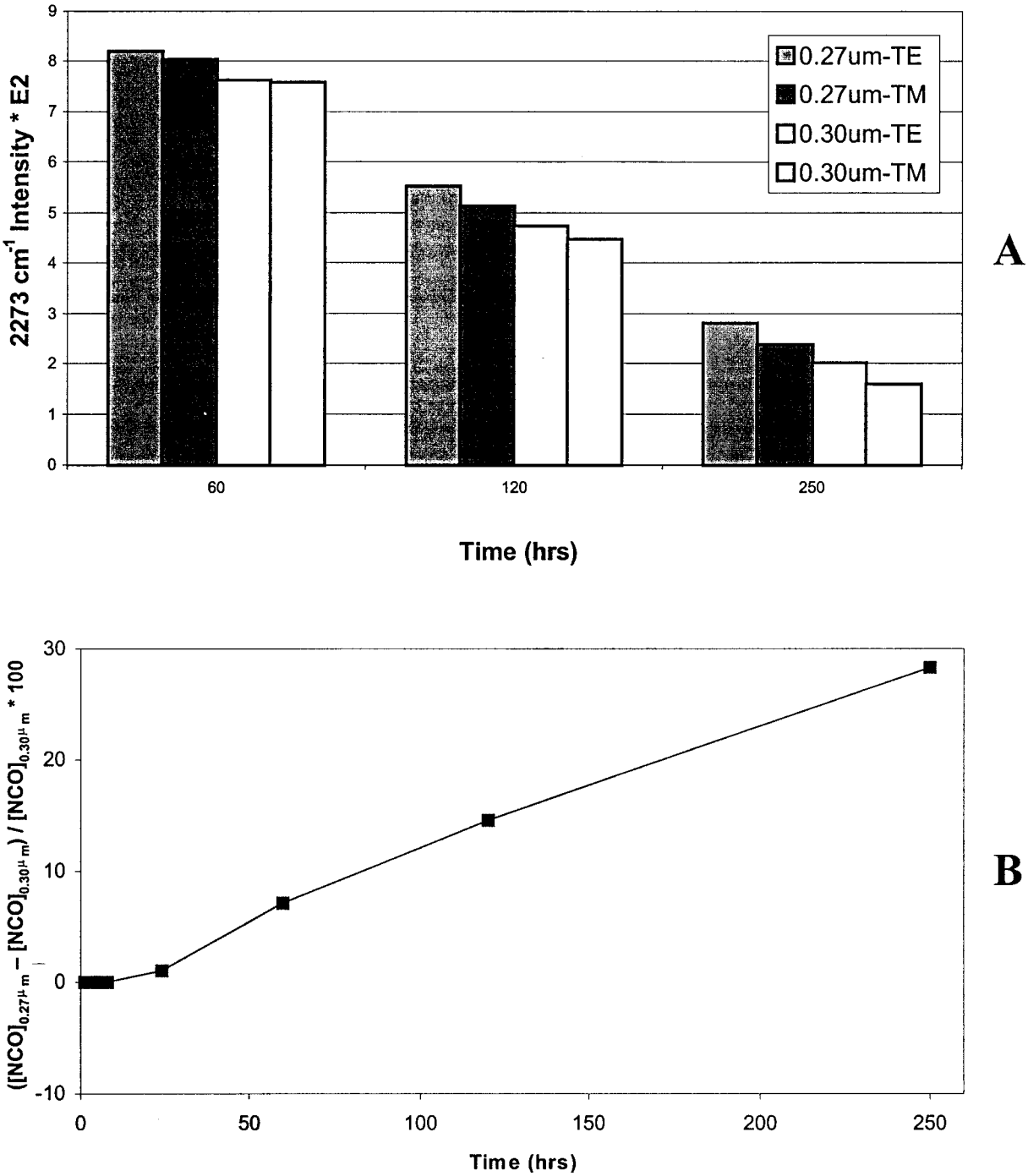

Figure 4 (A) NCO (2273 cm^{-1}) intensity as a function of reaction time recorded for TE and TM polarization at the F–S interface at later stages of crosslinking. (B) Relative change of NCO concentration at different depths of penetration (0.27 versus 0.30 μm) as a function of time.

polarization has an electric vector perpendicular to the crystal plane.[17] The spatial direction of these two polarizations thus allow us to distinguish between the dipole moment changes in the film plane and those oriented perpendicular to the plane. By superimposing TM and TE spectra recorded from the same penetration depth, we will be able to examine the preferential orientation of

the functional groups. Experiments showed that during the early stages of the reactions (up to 5 h) the NCO intensity at 2273 cm^{-1} does not change as a function of the penetration depth and direction. However, at the later stages, NCO groups show stratification and orientation preference. Figure 4(A) shows the NCO intensity changes near the F–S interface plotted as a function of time at the later stages of crosslinking based on the ATR spectra recorded using TM and TE polarizations. The enhanced intensity of the TE spectrum indicates that there are more C═O groups taking this orientation. Since the TE direction represents orientation parallel to the F–S interface, at a given time and depth, more NCO groups are oriented in the direction parallel to the film plane.

Quantitative analysis of the NCO concentration changes at extended reaction times is shown in Figure 4(B), which illustrates the relative NCO concentration changes from 0.30 to 0.27 μm depths of penetration, $([NCO]_{0.27\mu m} - [NCO]_{0.30\mu m})/[NCO]_{0.30\mu m}$. It appears that, at the later stages of crosslinking, the NCO concentration increases at shallower depths from the F–S interface and the NCO concentration difference between various depths gradually increases with time.

Due to their ability to form hydrogen bonding (H-bonding), carbonyl groups are an important functionality in PURs. The orientation of H-bonding entities, determined using polarized ATR FTIR spectra, is shown in Figure 5. Trace A gives the original TM spectrum, while trace B shows the deconvoluted spectrum of A after a maximum-likelihood spectral analysis was applied.[14] This approach is commonly utilized when band overlap does not allow us to resolve spectral features. In this case, the deconvoluted spectra were generated from the best estimation of a maximum probability approach by using physical information about spectral features and statistical knowledge of the unknown number of overlapping bands. It appears that the 1728 cm^{-1} band, due to the stretching mode of C═O groups in PUR, was recorded using TM polarization splits to two bands at 1730 and 1720 cm^{-1}. However, for the TE polarized spectrum recorded in the range of 0.85 to 1.53 μm from the F–S interface, there is no detectable band split after deconvolution. Since the bands at 1730 and 1720 cm^{-1} are due to free C═O and H-bonded C═O groups, respectively,[12] H-bonded C═O groups tend to align perpendicular to the F–S interface plane.

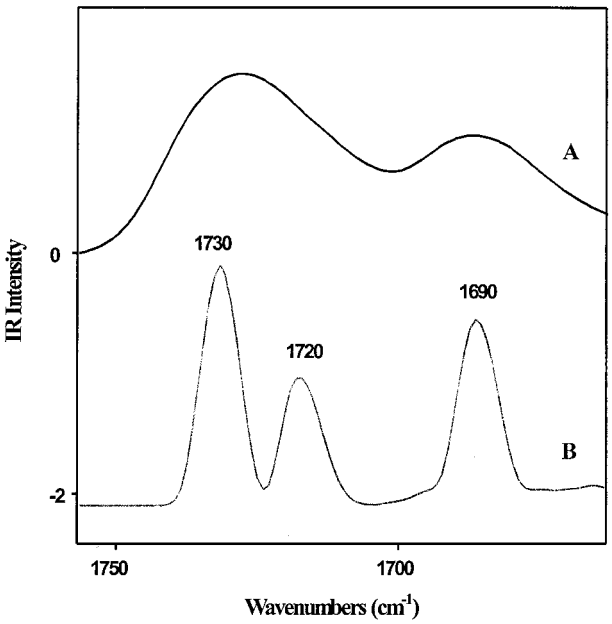

Figure 5 TM polarized ATR FTIR spectra of the carbonyl region of solvent-borne PUR recorded at 0.85 μm from the F–S interface after 44 h of reaction under 7% RH.

Relative amounts of H-bonding at different penetration depths are compared in Figure 6, where the relative amounts of H-bonded C═O groups are represented by the ratio of 1720–1730-cm^{-1} band areas. It appears that, as the distance from the F–S interface increases, the extent of H-bonding also increases. In PUR films, both OH and NH species can be hydrogen donors to form H-bonding. Since there are relatively small amounts of OH functionalities left after 8 days of film formation, the primary source of hydrogen donors comes from N—H groups. However, at shallower penetration depths, the situation changes, in which case there are H-bonded C═O groups in both parallel and perpendicular directions, although higher H-bonded C═O content is detected in the direction perpendicular to the F–S interface. Results of quantitative analysis at depths ranging from 0.36 to 0.40 μm are given in Figure 7. Although there is no significant difference in the total concentration fraction of H-bonded C═O with respect to penetration depths, more H-bonded C═O groups are oriented in the direction perpendicular to the F–S interface (TM). Thus, the results shown in Figures 7 and 8 indicate that the amount and orientation of H-bonded carbonyl groups vary with the penetration depth near the F–S interface, which is schematically summarized in Figure 8.

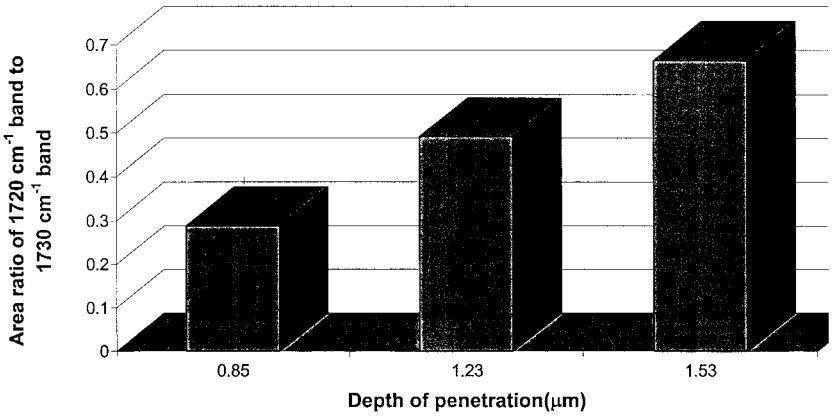

Figure 6 Area ratio of band at 1720 cm^{-1} to band at 1730 cm^{-1} of solvent-borne PUR at 0.85, 1.23, and 1.53 μm from the F–S interface after 200 h of reaction under 7% RH.

The formation of H-bonded species requires specific orientation and space between the hydrogen donors (N—H groups) and acceptors (C═O groups). If hydrogen donors and acceptors are located too far from each other, or if they are unable to assume a favorable orientation, H-bonding will not occur. However, as reactions proceed, the amount of H-bonding may change due to molecular relaxations. Figure 9 shows the area ratio of the 1720–1730-cm^{-1} bands recorded from 0.36-, 0.39-, and 0.40-μm depths near the F–S interface for TE and TM polarizations. As seen, the area ratio increases as a function of time. This information can be used to determine the transient behavior of H-bonded C═O groups by calculating the dichroic ratio of these bands.[18] Following a well-established convention, the dichroic ratio for an absorption band is defined by[19]

$$D = I_{\parallel}/I_{\perp} \tag{1}$$

where $I_{\parallel}$ and $I_{\perp}$ are band intensities of TE and TM polarized IR spectra, respectively.

The orientation of species is usually expressed by the Herman orientation F, which has the following relationship with the dichroic ratio:

$$F = (D_0 + 2)(D - 1)/(D_0 - 1)(D + 2) \tag{2}$$

where $D_0 = 2 \cot^2 \alpha$ and α is the angle between the transition moment of the vibration and the H-bonded C═O, which is assumed to be 0° for the C═O stretching band. Using the following relationship,

$$F = \langle 3 \cos^2\theta - 1\rangle/2 \tag{3}$$

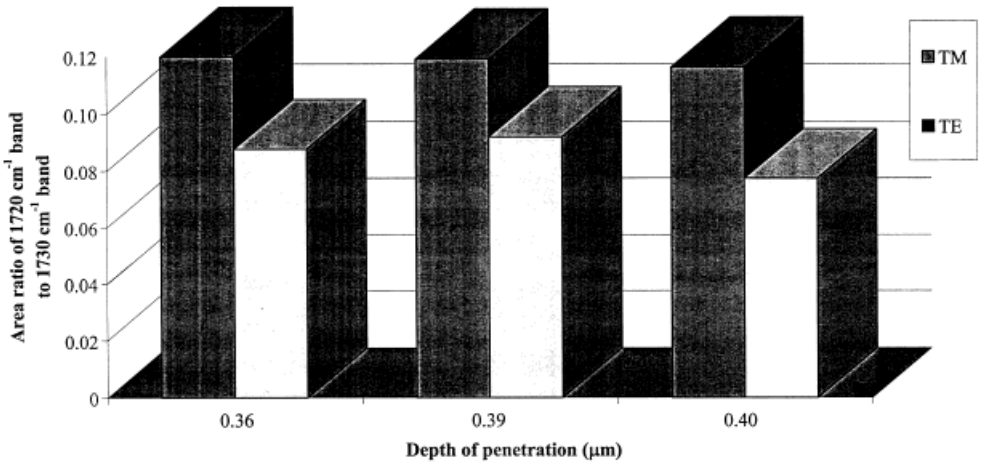

Figure 7 Area ratio of band at 1720 cm^{-1} to band at 1730 cm^{-1} of solvent-borne PUR at 0.36, 0.39, and 0.40 μm from the F–S interface after 200 h of reaction under 7% RH.

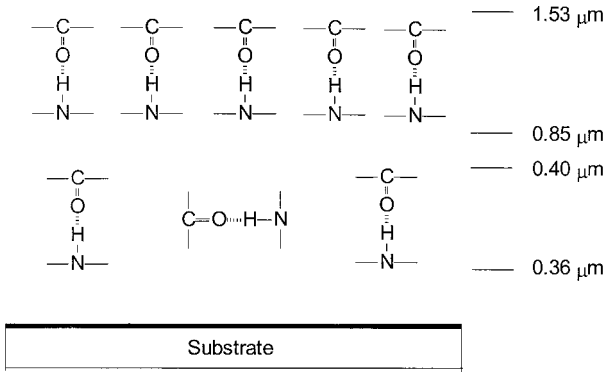

Figure 8 Schematic representation of hydrogen-bonded carbonyl group distribution and orientation.

the average orientation angle of H-bonded C═O, θ, can be determined. Figure 10 illustrates the orientation function F and an average angle θ's changes plotted as a function of time at penetration depths ranging from 0.36 to 0.40 μm. It appears that the average angle between H-bonded C═O and the F–S interface is about 60°, which slightly decreases with time, indicating that the orientation of H-bonded C═O groups becomes more random. It should also be pointed out that the majority of orientation changes occur at the early stages of crosslinking. As reactions progress, solvent evaporates and molecular segment motions result in additional H-bonding and the direction of H-bonded C═O groups becomes more random at extended reaction times. As we recall from data shown in Figure 2, which are inserted in Figure 10, it takes about 2 h for 60% of the solvent to evaporate; thus, the remaining portion will plasticize the urethane network and randomize orientation of the H-bonded C═O direction.

One issue that is also of interest is why the H-bonding direction changes as a function of the penetration depth. As seen from Figures 6(a) and 7(a), at deeper depths (0.85–1.53 μm), almost all H-bonded C═O groups take the perpendicular direction, indicating that local polymer segments preferentially align parallel to the F–S interface. However, at shallower depths (0.36–0.40 μm), H-bonded C═O groups also take other directions, indicating that some local segments take directions other than the parallel one. Experimental observation shows that there is a tendency for the urea structure to migrate to the F–S interface, which may cause randomization of molecular segment orientation. To address why the urea structure moves to the interface, interfacial tensions are estimated. The interfacial energy γ can be estimated based on the following relationship[20]:

$$\gamma_{ps} = \gamma_p + \gamma_s - 2(\gamma_p\gamma_s)^{1/2} \quad (4)$$

where the subscripts p and s denote the polymers and the substrate that form the interface.

Based on surface tensions of —NHCONH—, —NHCOO— entities and Ge,[21,22], the urea/Ge and urethane/Ge interfacial tensions are calcu-

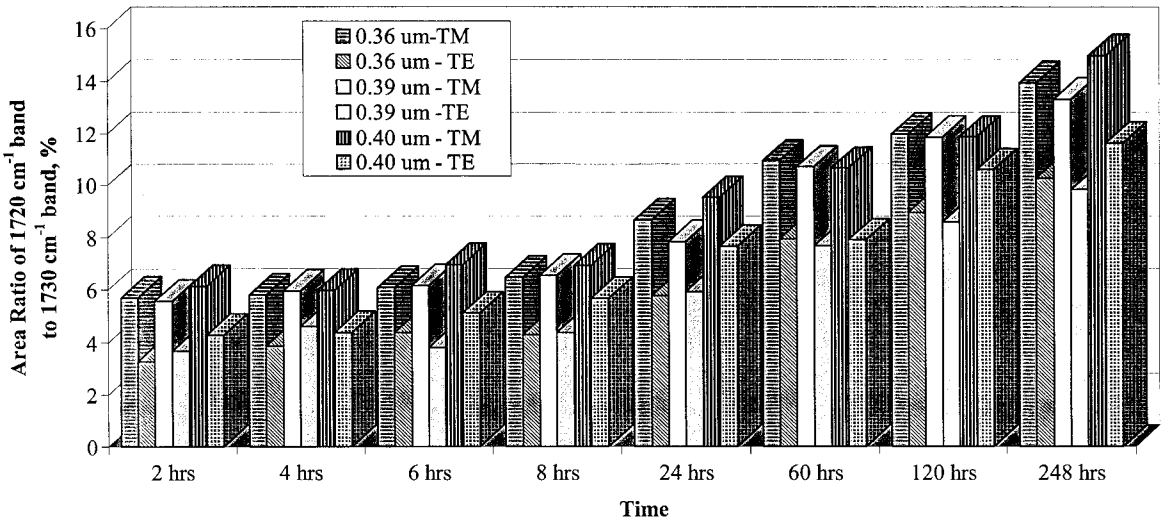

Figure 9 Area ratio of band at 1720 cm^{-1} to band at 1730 cm^{-1} of solvent-borne PUR as a function of reaction time recorded at 0.36, 0.39, and 0.40 μm from the F–S interface and TM and TE polarizations under 7% RH.

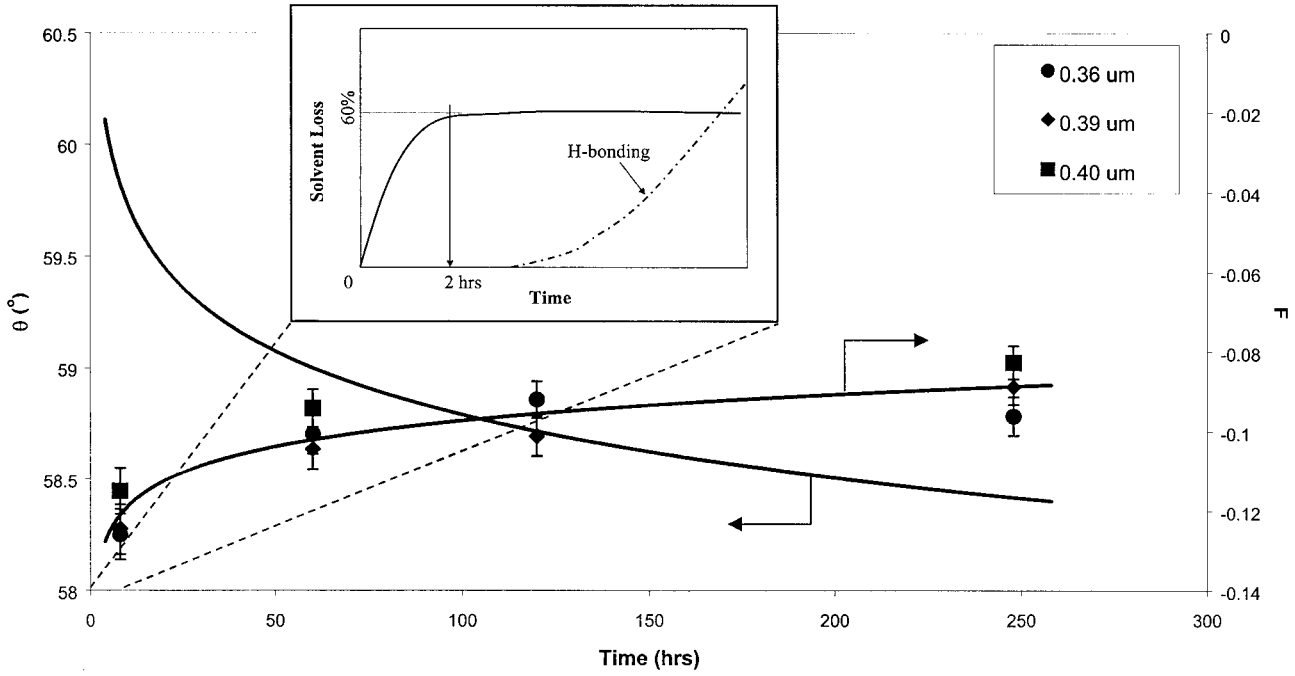

Figure 10 Orientation function (F) and average angle between H-bonded C═O bands and the F–S interface (θ) as a function of time.

lated to be 371 and 321 mN/m, respectively. Since the urea/Ge interface exhibits a lower interfacial tension, segments containing ureas migrate to the F–S interface, thus randomizing segmental orientation of layers near the F–S interface, As a consequence, H-bonding is reduced and random. Figure 11 schematically shows the orientation of H-bonding and local segments at various depth regions.

CONCLUSIONS

In summary, at the early stages of PUR crosslinking reactions, the NCO concentration changes due to solvent evaporation, resulting in a volume reduction of the film, and there is no stratification and no preferential orientation of NCO groups during this period. At the later stages of film formation, the NCO content near the F–S inter-

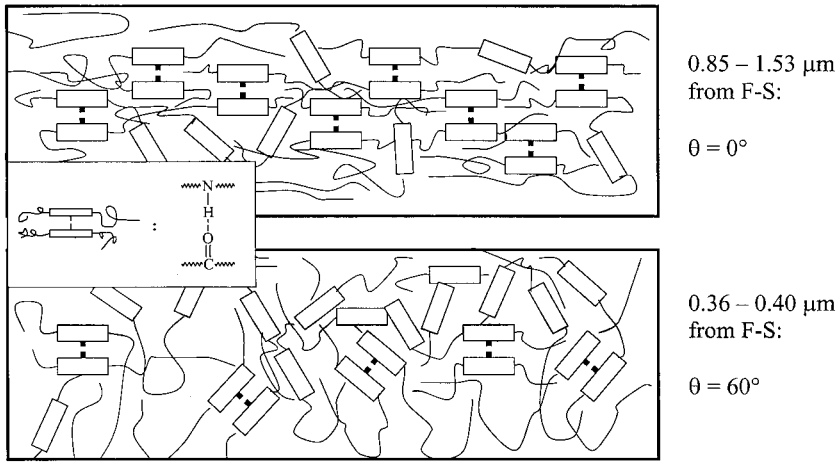

Figure 11 Schematic representation of H-bonding and local molecular segment orientation in a PUR film near the F–S interface.

face is higher and exhibits a preferentially parallel orientation with respect to the surface. The orientation of H-bonded C═O groups is preferentially perpendicular near the F–S interface, but they tend to take parallel orientation closer to the interface.

The authors are thankful to the National Science Foundation Industry/University Cooperative Research Center in Coatings and the Bayer Corp. for a financial support of these studies.

REFERENCES

1. Ludwig, B. W.; Urban, M. W. J Coat Tech 1994, 66(839), 59.
2. Coleman, M. M.; Skrovanek, D. J.; Hu, J.; Painter, P. C. Macromolecules 1988, 21, 59.
3. Srichatrapimuk, V. W.; Cooper, S. L. J Macromol Sci-Phys B 1978, 15, 267.
4. Claybourn, M.; Reading, M. J Appl Polym Sci 1992, 44, 565.
5. MacKnight, W. J.; Yang, M. J Polym Sci 1973, 42, 817.
6. Hobbs, J. P.; Sung, C. S. P.; Krishman, K.; Hill, S. Macromolecules 1983, 16, 193.
7. Ludwig, B.W.; Urban, M. W. J Coat Tech 1996, 68(857), 93.
8. Usmani, A. M. J Coat Technol 1984, 56(716), 99.
9. Bummer, P. M.; Knutson, K. Macromolecules 1990, 23, 4357.
10. Kaminski, A. M.; Urban, M. W. Polym Mater Sci Eng 1996, 74, 220.
11. Kaminski, A. M.; Urban, M. W. J Coat Tech 1997, 69(872), 55.
12. Kaminski, A. M.; Urban, M. W. J Coat Tech 1997, 69(873), 113.
13. Fluornoy, P. A.; Schaffer, W. J. Spectrochim Acta 1966, 22, 5.
14. Urban, M. W. Vibrational Spectroscopy of Molecules and Macromolecules on Surfaces; Wiley: New York, 1993.
15. Urban, M. W.; Allison, C. L.; Finch, C. C.; Tatro, B. A. J Coat Tech 1999, 71(888), 75.
16. Sung, C. S. P. Macromolecules 1981, 14, 591.
17. Fluornoy, P. A.; Schaffer, W. J. Spectrochim Acta 1966, 22, 5.
18. Tang, W.; MacKnight, W. J.; Hsu, S. L. Macromolecules 1995, 28, 4284.
19. Fraser, R. D. B. J Chem Phys 1956, 24, 89.
20. Bikerman, J. J. Physical Surfaces; Academic: New York, 1970.
21. van Krevelen, D. W; Hoftyzer, P. J. Properties of Polymers, Their Estimation and Correlation with Chemical Structure; Elsevier: Amsterdam, 1976.
22. CRC Handbook of Chemistry and Physics, 77th ed.; D. R. Lide, Ed.; CRC: Boca Raton, FL, 1996.